Published in final edited form as:
Int J Cancer. 2013 February 1; 132(3): 695–706. doi:10.1002/ijc.27687.

Oxidative inhibition of Hsp90 disrupts the super-chaperone complex and attenuates pancreatic adenocarcinoma *in vitro* and *in vivo*

Sayantani Sarkar[1], **Devawati Dutta**[1], **Suman Kumar Samanta**[1], **Kaushik Bhattacharya**[1], **Bikas Chandra Pal**[2], **Jinping Li**[3], **Kaustubh Datta**[4], **Chhabinath Mandal**[2], and **Chitra Mandal**[1]

[1]Cancer Biology and Inflammatory Disorder Division, Council of Scientific and Industrial Research-Indian Institute of Chemical Biology, Kolkata, India

[2]National Institute of Pharmaceutical Education and Research, Kolkata (at IICB-CSIR), Kolkata, India

[3]Department of Biomedical Science, Mercer University School of Medicine, Savannah, GA

[4]Department of Biochemistry and Molecular Biology and Eppley Cancer Center, University of Nebraska Medical Center, Omaha, NE

Abstract

Pancreatic cancer is almost always fatal, in part because of its delayed diagnosis, poor prognosis, rapid progression and chemoresistance. Oncogenic proteins are stabilized by the Hsp90, making it a potential therapeutic target. We investigated the oxidative stress-mediated dysfunction of Hsp90 and the hindrance of its chaperonic activity by a carbazole alkaloid, mahanine, as a strategic therapeutic in pancreatic cancer. Mahanine exhibited antiproliferative activity against several pancreatic cancer cell lines through apoptosis. It induced early accumulation of reactive oxygen species (ROS) leading to thiol oxidation, aggregation and dysfunction of Hsp90 in MIAPaCa-2. *N*-acetyl-L-cysteine prevented mahanine-induced ROS accumulation, aggregation of Hsp90, degradation of client proteins and cell death. Mahanine disrupted Hsp90-Cdc37 complex in MIAPaCa-2 as a consequence of ROS generation. Client proteins were restored by MG132, suggesting a possible role of ubiquitinylated protein degradation pathway. Surface plasmon resonance study demonstrated that the rate of interaction of mahanine with recombinant Hsp90 is in the range of seconds. Molecular dynamics simulation showed its weak interactions with Hsp90. However, no disruption of the Hsp90-Cdc37 complex was observed at an early time point, thus ruling out that mahanine directly disrupts the complex. It did not impede the ATP binding pocket of Hsp90. Mahanine also reduced *in vitro* migration and tube formation in cancer cells. Further, it inhibited orthotopic pancreatic tumor growth in nude mice. Taken together, these results provide evidence for mahanine-induced ROS-mediated destabilization of Hsp90 chaperone activity resulting in Hsp90-Cdc37 disruption leading to apoptosis, suggesting its potential as a specific target in pancreatic cancer.

Correspondence to: Chitra Mandal, Cancer Biology and Inflammatory Disorder Division, CSIR-Indian Institute of Chemical Biology, 4, Raja S.C. Mullick Road, Kolkata 700 032, India, Tel.: +91-33-2429-8861, Fax: +91-33-2473-5197, chitra_mandal@yahoo.com.

Additional Supporting Information may be found in the online version of this article.

Keywords

apoptosis; Cdc37; Hsp90; mahanine; pancreatic cancer; reactive oxygen species

Pancreatic cancer is the fourth leading cause of cancer-related death and 5-year survival rate is only 6%. The incidence and mortality rates are almost equal. Approximately 36,800 deaths were reported in the USA in 2010.[1] Because of its rapid progression, massive invasiveness, late diagnosis and intense resistance to any form of chemotherapy,[2] only 15–20% of patients with progressing pancreatic carcinoma are amenable to curative resection, while the rest have nonresectable, metastatic cancers. The multifaceted biological mechanisms underlying this disease remain mostly unknown.[3,4] At present, the mutation and/or overexpression of certain oncogenes (K-Ras, ErBb2, Akt, TGF-β, EGFR) and mutation, LOH or downregulation of tumor suppressor genes (p53, p16, BRCA2) are reported.[3] Reactive oxygen species (ROS) are generated primarily by the interaction of oxygen molecules with electrons that escape from the mitochondrial respiratory chain (MRC).[5,6] Inhibition of the activity of MRC complexes increases the leakage of electrons by blocking the electron transfer chain and promoting ROS accumulation.[6,7] A high level of ROS production beyond a certain threshold can result in oxidative damage of DNA, proteins and lipids.[8]

The molecular chaperone Hsp90 is highly expressed in cancerous cells and is essential for their survival, making it a potential chemotherapy target. It mediates the folding, assembly and maturation of many client proteins, including HER-2, EGFR, PI3K, Akt, B-Raf, Stat-3, GSK3β, Cdk4, mutated p53 and steroid receptors all of which are directly involved in malignant cancer.[9,10]

Herbal compounds have been shown to hold a great deal of promise as chemotherapeutic agents against a variety of cancers.[11,12] The purified carbazole alkaloid mahanine (Fig. 1*a*), isolated from the edible plants *Murraya koenigii* and *Micromelum minutum*, has been shown to possess antimutagenic, antimicrobial and cytotoxic activities.[13–16] Mahanine is a potent apoptosis inducer in histiocytic lymphoma, promylocytic leukemia[17,18] and prostate cancer cells.[19] We previously demonstrated that mahanine is a potential activator of the cellular death cascade in a leukemic model.[20] It is also an activator of the epigenetically suppressed tumor suppressor gene RASSF1A.[21] Despite its known function as an inducer of apoptosis, the intracellular protein targets of mahanine are presently unknown. The main objective of this study was to understand the underlying molecular mechanism of mahanine-induced apoptosis, so we focused on the role of reactive oxygen species and Hsp90 as potential regulatory target molecules of mahanine in pancreatic cancer.

Here we provide evidence for a pro-oxidant mediated assault on the Hsp90 pathway during mahanine-induced pancreatic ductal adenocarcinoma cell death. Mahanine-mediated ROS generation facilitates a disruption of the Hsp90-Cdc37 super-chaperone complex without hindering ATP binding. *In vitro* surface plasmon resonance (SPR) and *in silico* docking and molecular dynamics (MD) simulation revealed that mahanine can interact with Hsp90 and is in rapid equilibrium in solution. However, these interactions are through weak forces and are reversible in nature. Hence, they neither impede nor facilitate the disruption of the Hsp90-Cdc37 complex, which results as a downstream consequence of ROS generation at a longer time scale. To the best of our knowledge this is the first report of the involvement of mahanine-induced ROS in the Hsp90 dysfunction which leads to a subsequent disruption of the Hsp90-Cdc37 chaperone complex in pancreatic cancer.

Material and Methods

Purification and characterization of mahanine

Mahanine was purified from fresh leaves of a native Indian plant, *Murraya koenigii* belonging to the family *Rutaceae*.[19] The purity was confirmed by HPLC.[20] LC-MS, ^{1}[H] and ^{13}[C] NMR spectral data analysis established its structure as mahanine. Details are furnished in Supporting Information S-1.

Cell lines

Human pancreatic ductal adenocarcinoma cell lines, MIAPaCa-2, AsPC-1, Panc-10.05, Panc-1 and BxPC-3 (Supporting Information S-2, Table 1) were purchased from ATCC, authenticated by STR profiling with PowerPlex 16 HS system (Promega) using ABI 3130 Genetic Analyzer (Applied Biosystems) during 2009 at a coauthor's lab, in USA, and crosschecked with the ATCC data bank. All cells were grown in RPMI-1640 supplemented with 10% heat inactivated fetal bovine serum (FBS) and 1% antibiotic-antimycotic, in a humidified atmosphere at 37°C, with 5% CO_2.

Cell viability assay

Cells (1×10^4) were exposed to mahanine (0–50 μM) for 48 hr and consequently 3-(4,5-dimethylthiazol-2-yl)-2,5-diphenyl tetrazolium bromide (MTT, 100 μg per well) was added to fresh culture media and further incubated for 3 hr. Generated formazane crystals were dissolved in DMSO and optical density was measured at 550 nm in a spectrophotometer (Thermo Scientific, USA).[22] Control cells were exposed to the highest amount of the vehicle (0.15% absolute ethanol).

Intracellular ROS measurement

Cells were treated with mahanine for 0–24 hr (20 μM) and 1 hr (10–20 μM) and incubated with H_2DCF-DA (10 μM) for 30 min at 37°C. Intracellular H_2O_2 was determined using flow cytometry, by analyzing 10,000 cells with CellQuest Pro software (BD FACSCalibur). For ROS inhibition, the experiment was repeated with *N*-acetyl-L-cysteine (NAC, 2.5 mM) pretreatment for 1 hr.[23]

Immunoblot, immunoprecipitation and immunohistochemistry

Cells (1×10^6) were treated with mahanine (0–20 μM) for 24 hr and 50 μg of proteins were separated in SDS-PAGE (7.5–12.5%) followed by electrotransfer into nitrocellulose membrane, blocked with TBS-BSA, probed overnight with primary antibodies (S-1) and washed with 0.1% Tween-20 containing TBS. Immunocomplexes were identified with HRP-conjugated secondary antibodies. The membrane was washed and target proteins were identified by the West-pico ECL system (Pierce, Thermo Scientific, USA).

For detection of the chaperone complex, whole-cell lysate (350 μg) was incubated with anti-Hsp90 antibody (1:100) overnight at 4°C followed by further incubation with Protein A-Sepharose 4B. The immunocomplex was resolved by nonreducing SDS-PAGE and subsequently identified using the respective antibodies.

For immunohistological staining, cryo-preserved tumors were fixed, embedded in paraffin and microtome-sectioned. Tissue sections were stained by anti-Akt and anti-Stat-3 antibodies.

Nonreducing SDS-PAGE for detection of ROS-dependent chaperone proteins

For analysis of oligomerization of Hsp90, mahanine-treated (10 and 20 μM, 24 hr) cells in the presence or absence of NAC (2.5 mM, 1 hr) were processed.[24] Samples were resolved in SDS-PAGE in the absence of β-mercaptoethanol and detected by Western blot analysis using anti-Hsp90 antibody.

Surface plasmon resonance analysis

Carboxymethyl-dextran sensor chips (CM) were equilibrated with running buffer (10 mM HEPES, pH 7.4, 0.15 M KCl and 0.001% Tween20) to prevent any nonspecific binding of proteins to the capillaries of the BIAcore apparatus for a period of 10 min at 25°C at a flow rate of 5 μl min^{-1}. The CM chip was activated with 1-ethyl-3-[3-dimethylaminopropyl]-carbodiimide (200 mM) and *N*-hydroxy-succinamide (50 mM) for 5 min at 25°C. Human recombinant Hsp90 protein (20 μg) was dialyzed against coupling buffer-1 (5 mM Na_2HPO_4, pH 7.4 and 150 mM NaCl) at 4°C.[25,26] The dialyzed protein was coupled with a chip in buffer-2 (20 mM Na-acetate, pH 4.0) for 10 min at 25°C. Noncovalently bound Hsp90 was removed by two brief fluxes (2 min) of HCl (20 mM). Mahanine (0.5–30 μM) was injected onto an Hsp90 coated CM5-sensor chip at a flow rate of 10 μl min^{-1}. Rebinding, at a flow rate of 5 μl min^{-1}, and mass transfer were also checked by the repetition of the experiments with lower levels of immobilized recombinant Hsp90. 17-AAG was used as a positive control.

ATP-Sepharose binding assay

Human recombinant Hsp90α and Hsp90β (5 μg) proteins were treated with mahanine (50–100 μM) in incubation buffer [200 μl, 10 mM Tris–HCl, 50 mM KCl, 5 mM $MgCl_2$, 2 mM DTT, 20 mM Na_2MoO_4, 0.01% NP-40, pH 7.5] at 4°C for 30 min. Pre-equilibrated γ-phosphate-linked ATP-Sepharose (25 μl) was added and incubated at 37°C for another 30 min. The bound complex was washed, resolved in SDS-PAGE and detected by Western blot analysis using an anti- Hsp90 antibody. The 17-AAG and ethanol were used as positive and negative controls, respectively.[27]

Molecular modeling studies

The details on the computational studies are provided in the Supporting Information S-3, A–D. In brief, the structural coordinates of the human Hsp90 and Cdc37 proteins were obtained from the NMR-derived structure of the complex in the Protein Data Bank (2K5B). Mahanine was constructed and optimized using the molecular modeling software suite Insight II (2005) of Accelrys (San Diego, CA, S-3-A).[28] Molecular docking of the optimized mahanine structure to human Hsp90 was performed using Autodock 4.2 (S-3-B).[29] Two molecular dynamics (MD) simulations were performed using the Gromacs-3.3.2 package applying the GROMOS96 force field, one being the ligand-protein complex and the other the ligand free in solution (S-3-C),[30,31] to evaluate the absolute binding energy of the ligand-receptor complex. The parameterization of the ligand was carried out in the Dundee PRODRG server using the GROMOS96 force field.[32] Trajectories and simulated structures were analyzed using VMD software.[33] The free energy of the binding of ligand to the protein was calculated using the linear interaction energy (LIE) method (S-3-D).[34–36] The binding free energy (ΔG_{bind}) value was used to calculate the binding dissociation constant (K_D). The molecular visualization of the structures was performed using PyMol.[37]

Scratch-wound assay

Highly invasive (MIAPaCa-2) and moderately invasive (BxPC-3) pancreatic cancer cells (1×10^6/ml/well) were cultured to >90% confluency. Subsequently, cells were starved in reduced-serum (0.5%) media overnight. Three separate scratch-wounds were then made and

cells were provided with reduced-serum media containing successive doses of mahanine for 6 hr. Images were taken using phase-contrast microscopy.[38]

Transmigration assay

MIAPaCa-2 cells were treated with mahanine (10–20 μM) for 24 hr. VEGF, EGF and PDGF were subsequently added into the outer well of the 24-transwell plate (PromoCell Heidelberg, Germany) at a final concentration of 20 ng ml^{-1}. Mahanine-pretreated cells (5×10^4 cells/well/500 μl) were added into the insert and incubated for 6 hr. Subsequently, invader cells were fixed with chilled methanol and stained with 0.1% crystal violet. Random fields were photographed and quantified under phase contrast microscopy.

Orthotopic pancreatic tumor model

A new MIAPaCa-2-derived cell line was developed stably expressing the luciferase gene. Luciferase expression had been previously verified to be at a satisfactory level for noninvasively imaging the tumor in animal experiments. Thirty-five mice, female, nu/nu athymic, 4–6 weeks old, were obtained from Harlan Laboratories. The pancreas of anesthetized mice was exposed through a midline laparotomy incision and retraction of the spleen. Cells (1×10^6, 50 μl RPMI-1640) were injected directly into the pancreas. It took 8 days for the mice to develop the pancreatic tumor. Consequently, the uniform volume of the pancreatic tumor was confirmed by *in vivo* bioluminescent imaging prior to treatment (Supporting Information Fig. S-10). Accordingly, twenty-eight mice were randomly clustered in the two following groups ($n = 14$ in each group); untreated vehicle control and treated (i.p., 100 mg/250 μl mahanine/kg/day) for 12 successive days. All mice were sacrificed on Day 13, following the last dose of treatment and their body weight was measured. Subsequently, tumors and the pancreas were excised from each mouse in both groups and their weights were determined.

Statistical analysis

Data were from at least three independent experiments. Statistical analysis was performed using the two-tail Student *t* test. Error-bars represent the standard deviation of the mean (±SD). Significant differences ($p < 0.05$) between the means of the control and mahanine-treated cells or two test groups were analyzed by Microsoft Excel and Graph pad Prism.

Results

Mahanine exhibits antiproliferative effects in an array of pancreatic cancer cells

To determine the efficacy of mahanine against pancreatic cancer, the compound was tested for cytotoxicity against an array of pancreatic cancer cells using the MTT assay. Mahanine treatment for 48 hr resulted in a dose-dependent decrease in cell viability in all of the four pancreatic carcinoma cell types with different grades of disease[39] (S-2). It displayed a cytotoxic effect against the gemcitabine-resistant cells MIAPaCa-2, AsPC-1, Panc-10.05 and Panc-1, with IC_{50} values of 13.9, 16.5, 17.2 and 18.5 μM, respectively (Fig. 1*b*). Ethanol (0.15%) served as the vehicle control and exhibited a minimal adverse effect. Both normal human lung fibroblast cells (WI-38) and African green monkey kidney cells (Vero) exhibited a minimal effect, even at a 50 μM dose (Supporting Information Fig. S-4).

Mahanine induces apoptosis in MIAPaCa-2 cells

To examine whether mahanine-induced cell death was due to apoptosis, we investigated its effect on caspases and poly-ADP ribose polymerase (PARP) in terms of their protein levels. Western blot analysis revealed that effector caspases, specifically caspase-7 and caspase-3, were activated at a 12.5 μM dose of mahanine after 24 hr of incubation. It is believed that

PARP is inactivated by effector caspase activation.[40] Cleavage of PARP became significant at a 15 μM dose of mahanine after 24 hr (Fig. 1*c*).

Early accumulation of ROS and its effects on cytotoxicity

It was previously demonstrated that mahanine induces ROS in leukemic cells.[18,20] To further elucidate whether mahanine induces pro-oxidants in MIAPaCa-2, ROS production was assessed. Mahanine (20 μM)-treated MIAPaCa-2 exhibited significantly enhanced intracellular ROS levels within 30 min, which remained elevated for up to 2 hr. In parallel, 17-AAG (1 μM), a known Hsp90 inhibitor used as positive control, also exhibited its highest ROS accumulation within 30 min (Fig. 2*a*). Dose-dependency assay also confirmed that mahanine increased the pro-oxidant level within 1 hr, even at 15 μM (Fig. 2*b*). Pretreatment with the glutathione precursor NAC, successfully decreased the mahanine- and 17-AAG-induced ROS levels (Figs. 2*a* and 2*b*). Additionally, NAC also rescued the effects of mahanine-induced cell death to a level of ~72% after 24 hr (Fig. 2*c*). Phase contrast microscopy also confirmed that preincubation with NAC restored cellular morphology to almost 90% after 12 hr of mahanine incubation (Supporting Information Fig. S-5).

Oxidation of chaperone proteins is induced by mahanine

Because chaperone proteins are highly susceptible to ROS,[24] we investigated mahanine-induced ROS-dependent oxidation of Hsp90. After a 24-hr mahanine treatment, MIAPaCa-2 cells exhibited a dose-dependent increase in disulfide-linked Hsp90. This is suggested by the altered mobility of a considerable amount of Hsp90 protein, under nonreducing conditions, detected as bands shifted to higher molecular weight locations. However, accumulation of disulfide-linked Hsp90 after mahanine-treatment could be detoxified by subsequent NAC incubation suggesting involvement of ROS (Fig. 2*d*).

Degradation of Hsp90 client proteins and their restoration by NAC suggest a critical role of ROS

After successfully demonstrating that mahanine exerts potent cytotoxicity against pancreatic cancer cells, and that it induces apoptosis of MIAPaCa-2 cells and elevates the intracellular ROS level leading to oxidation of the chaperone protein Hsp90, we further investigated whether it inhibits Hsp90 functions. The expression of an array of its client proteins was evaluated both in MIAPaCa-2 and AsPC-1. Mahanine exhibited a dose-dependent decrease of a number of client proteins, including Akt, B-Raf, Stat-3, A-Raf, mutated p53, GSK3β and PKCβ at 24 hr in MIAPaCa-2 and AsPC-1 up to a dose of 30 μM (Supporting Information Fig. S-6).

Additionally, to monitor the efficacy of mahanine at lower (10–20 μM) doses, we treated MIAPaCa-2 for 24 hr. Mahanine exhibited a downregulation of client proteins even at lower doses. After incubation for 24 hr, mahanine was able to decrease the protein level of Akt and CDK-4 significantly at 15 μM, while B-Raf, Stat-3 and Bcl-X_L were notably decreased at 17.5 μM (Fig. 2*e*). In parallel, we checked the status of an Hsp90 nonclient protein (Cyclin E), which did not show any significant decrease, even at a 20 μM dose for 24 hr.

We also examined whether prevention of chaperone protein oxidation by NAC would lead to a reduction in mahanine-induced client protein degradation in MIAPaCa-2 cells. Mahanine (20 μM) did not induce any significant decrease in client proteins (Akt and B-Raf) within 6 hr (Fig. 2*f*). This time period may not be adequate to exhibit the efficacy of signal. However, a significant decrease of these client proteins was observed after 24 hr treatment. NAC pretreatment (1 hr) was able to rescue these client proteins (Fig. 2*f*).

Mahanine induces degradation of Hsp90 client proteins via the proteasome

Because most Hsp90 inhibitors result in client protein degradation *via* the proteasome, we were keen to examine whether mahanine also did so. Preincubation of MIAPaCa-2 with a 26S proteasome inhibitor (MG132, 10 μM for 1 hr) followed by a 24-hr mahanine (20 μM) treatment was enough to noticeably rescue the client proteins Akt, B-Raf, Stat-3, GSK-3β and Bcl-xL (Supporting Information Fig. S-7A). Interestingly, enhancement of the severity of insult by increasing the dose of mahanine from 20 μM to 30 μM did not significantly degrade many of the client proteins even after 6 hr of treatment, and those degraded were restored by MG132-preincubation in MIAPaCa-2 (Supporting Information Fig. S-7B).

Differential regulation of Hsp90 cochaperones supports the role of oxidative stress

Because Hsp90 and its cochaperones form a super-chaperone complex taking part in the cellular chaperone activities of protein folding and stabilization, we further investigated the status of other cochaperones after mahanine-treatment. Most of the well-characterized Hsp90 inhibitors also induce ROS, and hence, hinder its chaperone activities.[41–43] These Hsp90 inhibitors also potentially up-regulate Hsp70.[24] Mahanine (15 μM) upregulates Hsp70 and Hsp40 at a 17.5 μM dose. Therefore, it may be envisaged that these chaperones try to manage the unfolded protein load of the cell after pharmacological inhibition of Hsp90 by mahanine. Interestingly, no change was found in the Cdc37 total protein level. However, a cochaperone (p23) related to steroid receptor recruitment to Hsp90 was downregulated, with its cleaved form (p19) increasing in a dose-dependent manner (Fig. 3*a*).

Mahanine destabilizes Hsp90-Cdc37 interaction

Next, we wanted to study the interaction of Hsp90 with its cochaperones to unravel whether there was any mahanine-mediated destabilization of this super-chaperone complex. Significant down-regulation of Cdc37 was observed at 15 μM in 24 hr mahanine-treated cells, as was made evident in immunoprecipitation experiments followed by immunoblot analysis, although HOP and Hsp90 displayed almost the same levels with the IgG used as a loading control. Conversely, the pattern of p23 association with Hsp90 remained the same as it was in the total cell lysate (Fig. 3*b*). It is more likely that mahanine results in an indirect cleavage and downregulation of p23, therefore, reducing its presence in the super-chaperone complex.

Subsequently, we wanted to determine whether this Hsp90-Cdc37 destabilization was due to early ROS accumulation. No alteration of the Hsp90-Cdc37 chaperone complex was observed after incubation of MIAPaCa-2 with mahanine for 10–60 min, suggesting that ROS generation at a 20 μM dose did not hamper this complex formation at an early time point (Fig. 3*c*). This strongly suggests that the disruption of the Hsp90-Cdc37 complex is a downstream consequence of ROS generation.

SPR studies show weak affinity of mahanine to recombinant Hsp90

It is reported that Hsp90 inhibitors such as 17AAG and celastrol, which also generate ROS, bind Hsp90 directly.[41–43] Therefore, we used SPR to check interaction of mahanine with purified recombinant Hsp90. The portion of the sensor-gram which corresponds to the dissociation of mahanine from Hsp90 was analyzed to obtain the dissociation rate (k_d) (Fig. 3*d*). The experimental data is a good fit with the single exponential kinetic model used. Using the corresponding k_d values, nonlinear curve fitting of the association phase of the corresponding sensor-gram was carried out to obtain the association rate (k_a). The dissociation constant (K_D) for the Hsp90-mahanine complex was calculated as the ratio of the backward (6.21×10^{-3} S^{-1}) and forward (1.24 S^{-1}) rates (k_d/k_a) to obtain the value of

4.99 μM with maximum resonance (R_{max}) at 198.90. The 17-AAG was used as positive control (Supporting Information Fig. S-8).

Mahanine does not affect the ATP binding of Hsp90

The next aim was to determine whether mahanine disrupts the binding of ATP with Hsp90. The ATP-Sepharose binding assay demonstrated that the binding of mahanine with two purified isoforms of Hsp90 (Hsp90α and Hsp90β) did not block the ATP-binding pocket of Hsp90, whereas 17-AAG, a known ATP-binding inhibitor of Hsp90, did significantly block ATP binding under identical experimental conditions (Fig. 3*e*).

Molecular modeling reveals weak interactions of mahanine with recombinant Hsp90

Molecular docking revealed that mahanine did bind to Hsp90, through noncovalent weak interactions, in a polar groove, which was distinct from the ATP-binding cavity (Figs. 4*a* and 4*b*). Mahanine formed two hydrogen bonds with Hsp90, one with the side chain oxygen of Glu47 through its NH group and the other with the side chain oxygen of Asn51 through its OH group. In addition, it was shown that there were van der Waals interactions with Arg46, Ile43, Gly132, Gln133, Met130, Ser129, Phe138, Ile131 and Gly137 (Fig. 4*c*). The most favorable configuration of the ligand with the protein had a binding energy of −7.6 kcal mol^{-1}, with a micromolar binding affinity (K_D = 3.16 μM).

Mahanine inhibits pancreatic adenocarcinoma cell haptotaxis in a dose-dependent manner

A number of Hsp90 client proteins are associated with cell motility and invasion.[44] In a scratch wound haptotaxis assay, both the highly invasive MIAPaCa-2 and moderately invasive BxPC3[39] cells completed >40% wound closure within 6 hr in the vehicle control (Fig. 5*a*). In contrast, mahanine (20 μM)-treated cells exhibited ~95% wound closure inhibition.

Mahanine inhibits the in vitro migration of highly invasive pancreatic carcinoma cells

The migration of MIAPaCa-2 cells was inhibited after a 6-hr exposure to mahanine. At a 10 μM concentration of mahanine, epidermal growth factor (EGF)-driven MIAPaCa-2 migration was reduced to 48.6% of control, whereas nearly complete inhibition of cell migration was observed at a 15 μM dose (Fig. 5*b*). PDGF and VEGF-mediated MIAPaCa-2 chemo-migration exhibited an almost identical pattern, in which cell migration was a little more modest than that of the EGF-mediated one (data not shown).

Matrix metalloproteinases (MMPs) play a crucial role in cell motility. In particular, MMP-2 and MMP-9, which are Hsp90 client proteins, functionally control invasion and metastasis in malignancy. In this context, we observed that MMP9 was significantly down-regulated in mahanine-treated MIAPaCa-2 cells (Fig. 5*c*). The evident decrease of both the pro- and activated MMP9 further assured the anti-metastatic activity of mahanine.

Mahanine also inhibited the *in vitro* colony formation of MIAPaCa-2 cells on matrigel in a concentration-dependent manner within 24 hr (Supporting Information Fig. S-9*a*). There was ~80% inhibition of colony formation at the 10 μM dose. In contrast, no colonies were observed at the 15 μM dose or after 72 hr of mahanine (20 μM) incubation. Moreover, *in vitro* tubular differentiation assays showed that mahanine-treated MIAPaCa-2 cells were differentiated after a 3-day (3D) culture in matrigel in a dose-dependent manner (Supporting Information Fig. S-9*b*).

Mahanine inhibits tumor growth in an orthotopic mouse model

To further investigate mahanine activity in a pancreatic orthotopic nude mouse model, we implanted MIAPaCa-2 cells as an orthograft into the pancreas of nude mice to examine the *in vivo* efficacy of mahanine. *In vivo* bioluminescent imaging revealed the establishment of an even volume of tumor burden. A few representative mice are shown in Figure 6*a*. Mahanine (100 mg/kg/day) was administered intraperitoneally, and comprehensively inhibited tumor growth, resulting in reduced tumor volume after 12 days of consecutive treatment (Fig. 6*b*). We also observed that the tumor burden in mahanine-treated mice was significantly ($p < 0.05$) less than the one in the vehicle-treated controls. The pancreatic tumor load was represented as the weight of the excised pancreatic tumor in both the vehicle control and treatment groups, where $n = 14$ in each group (Fig. 6*c*). Immunostaining of the vehicle controls and mahanine-treated tumors also revealed a clear depletion of the two Hsp90 client proteins Akt and Stat-3 in this orthograft pancreatic adenocarcinoma mouse model (Fig. 6*d*).

Discussion

The present investigation of a novel cancer treatment focuses on the development of targeted therapy to specific oncogenic processes and related signaling pathways. Human pancreatic cancer is heterozygous in nature, comprising various genetic and epigenetic abnormalities which lead to uncontrolled cell proliferation, coupled with homozygous deletion of certain tumor suppressor genes. The chaperone Hsp90 has attracted considerable attention as a promising target as it is significantly upregulated in pancreatic carcinoma compared to normal tissue and regulates the function of several oncogenic proteins.[45] Although at present a few Hsp90 inhibitors are in clinical trials, none have come to market due to toxicity and solubility problems.

In this study we demonstrated the anticancer efficacy of a nontoxic novel carbazole alkaloid, mahanine, obtained from an edible plant, against pancreatic cancer. Mahanine-treatment significantly inhibited the proliferation of pancreatic cancer cells *in vitro* and also showed growth inhibition in orthotopic pancreatic tumor bearing immune-deficient mice. The main achievement of this study is the supply of evidence that mahanine drastically increases intracellular ROS, which leads to an oxidative insult of Hsp90. SPR revealed that mahanine reversibly binds to recombinant Hsp90 with faster kinetics of the order of seconds and exhibits a low binding affinity ($K_D = 4.99$ μM) in comparison with other known Hsp90 inhibitors.[41–43] This is in good agreement with the dynamic simulation value ($K_D = 3.16$ μM).

Hsp90 is a critical mediator of protein folding and maintains folded proteins in their proper conformation. Its expression level is reportedly high in cancer cells as compared to the noncancerous ones.[46] This comprehensive investigation revealed a critical role of mahanine-induced oxidative stress leading to oxidative insult of Hsp90, which further leads to a disruption of the Hsp90-Cdc37 complex, a cytotoxic effect against pancreatic cancer (Supporting Information Fig. S-11).

We reported previously that mahanine induced apoptosis in acute lymphoid cells (MOLT-3) by activating Fas/FasL.[20] The addition of a glutathione (GSH) precursor, NAC has been reported to increase cancer cell resistance to this carbazole alkaloid.[18,20] Whether mahanine-mediated ROS generation plays a role in the activation of this death receptor cascade, remains to be investigated in MIAPaCa-2. Mahanine-mediated Akt down-regulation in MIAPaCa-2 cells is also consistent with the result observed in prostate cancer cells.[19] However, the association between mahanine-mediated activation of the epigenetically

silenced tumor-suppressor gene RASSF1A[21] and ROS-induced Hsp90 inhibition is yet to be explored.

It is reported that chaperones are oxidation-sensitive proteins that are able to form disulfide bonds in response to various oxidative insults.[24] We showed that an early accumulation of ROS in mahanine-treated cells led to the oxidation of Hsp90. Nonreducing SDS-PAGE established that mahanine caused the formation of disulfide-linked high molecular weight conformers of Hsp90, indicating an oxidative assault on this chaperone protein. However, NAC scavenged these pro-oxidants and inhibited mahanine-induced cell death, which was also reflected in cellular morphology. This result clearly established that mahanine is a ROS-mediated inhibitor of the Hsp90 chaperone machinery. Therefore, unlike 17-AAG,[47] mahanine exhibited its activity independent of NQO1 expression, as MIAPaCa-2 cells [high NAD(P)H dehydrogenase quinone 1 (NQO1)] and Panc-1 cells [low NQO1] are similarly sensitive to this compound, pointing to different mahanine and 17-AAG mechanisms of action.

The functional activity of Hsp90 which was inhibited by mahanine treatment was attributed to the downregulation of its client proteins. A 6-hr mahanine treatment did not show any significant decrease in client protein level, although ROS accumulation occurred within 30 min. This supports a time lapse between the initial insult and its further intracellular effects. However, client-protein degradation after a 24-hr mahanine-treatment and its reversal by NAC preincubation established the critical role of ROS. NAC restores GSH which results in a decrease of the oxidative insult, allowing re-association of Hsp90 with its client proteins.

In this study, it was demonstrated that mahanine-induced ROS production leads to Hsp90 dysfunction. Some of the known Hsp90 inhibitors, such as geldanamycin and celastrol, were recently reported to have pro-oxidant activity.[41–43] The different status of the cochaperones after mahanine treatment further supported this observation. The upregulation of the Hsp70 and Hsp40 is a hallmark of Hsp90 inhibition, and was exhibited by mahanine treatment. However, the Cdc37 total protein level remained the same throughout the mahanine dose range, even though its association with Hsp90 dramatically decreased. This observation points toward the fact that mahanine also can disrupt the Hsp90-Cdc37 complex formation downstream of ROS generation. The expression level of the cochaperone p23 was decreased, while its cleaved form p19 increased, both in a dose-dependent manner. This observation is in agreement with a previous report that ER stress can lead to caspase-mediated cleavage of p23.[48] Mahanine-mediated activation of caspase-3 was initiated at the same dose at which cleavage of p23 was observed. It may be that unfolded protein response-mediated ER stress may also direct the cells towards apoptosis. Preliminary experiments suggested mahanine to be a Ca^{2+} channel inducer, and leakage of the intracellular Ca^{2+} pool is indicative of ER stress (unpublished observation).

Moreover, here, it was evinced that the observed mahanine-induced proteasome-dependent Hsp90 client protein degradation was mediated by the disruption of the Hsp90-Cdc37 complex. Mahanine was also shown to induce mitochondrial apoptosis through caspase activation.[18–20] Moreover, we demonstrated that, unlike 17-AAG, mahanine does not inhibit the Hsp90 chaperone activity by blocking ATP binding, whereas functional assays established that mahanine treatment reduces *in vitro* cell migration, colony formation and tubular differentiation in pancreatic carcinoma.

In conclusion, the herbal compound mahanine is able to potently induce a ROS-mediated oxidative assault on Hsp90 which disrupts the Hsp90-Cdc37 super-chaperone complex without hindering its ATP binding activity (Supporting Information Fig. S-11). Mahanine was demonstrated to possess *in vivo* anti-tumorigenic efficacy in an orthotopic nude mouse

model, and thus is a potential therapeutic agent targeting Hsp90 in human cancers. To the best of our knowledge, this is the first report on the cellular mechanism by which mahanine exerts its effects, and the findings may help put the treatment of the poorly manageable pancreatic adenocarcinoma into a broader perspective.

Supplementary Material

Refer to Web version on PubMed Central for supplementary material.

Acknowledgments

The authors sincerely acknowledge Prof. Siddhartha Roy, Director, CSIR-IICB, for his helpful comments and criticism. We also acknowledge Pacific Edit for providing their service in the manuscript editing.

Grant sponsor: CSIR-IICB, CSIR; Grant numbers: IAP-0001, HCP004; **Grant sponsor:** NMITLI; **Grant number:** TLP-004; **Grant sponsor:** DBT; **Grant number:** GAP 235; **Grant sponsor:** NIH; **Grant number:** R01 CA140432; **Grant sponsor:** American Cancer Society Research Scholar Grant; **Grant number:** RSG-07-044; **Grant sponsors:** J.C. Bose Fellowship, DST of Govt. of India, ICMR, German Cancer Research Center

References

1. Wang Z, Ahmad A, Li Y, et al. Targeting notch to eradicate pancreatic cancer stem cells for cancer therapy. Anticancer Res. 2011; 31:1105–1113. [PubMed: 21508353]
2. Niederhuber JE, Brennan MF, Menck HR. The National Cancer Data Base report on pancreatic cancer. Cancer. 1995; 76:1671–1677. [PubMed: 8635074]
3. Bardeesy N, DePinho RA. Pancreatic cancer biology and genetics. Nat Rev Cancer. 2002; 2:897–909. [PubMed: 12459728]
4. Li D, Xie K, Wolff R, Abbruzzese JL. Pancreatic cancer. Lancet. 2004; 363:1049–1057. [PubMed: 15051286]
5. Poyton RO, Ball KA, Castello PR. Mitochondrial generation of free radicals and hypoxic signaling. Trends Endocrinol Metab. 2009; 20:332–340. [PubMed: 19733481]
6. Li N, Ragheb K, Lawler G, et al. Mitochondrial complex I inhibitor rotenone induces apoptosis through enhancing mitochondrial reactive oxygen species production. J Biol Chem. 2003; 278:8516–8525. [PubMed: 12496265]
7. Dias N, Bailly C. Drugs targeting mitochondrial functions to control tumour cell growth. Biochem Pharmacol. 2005; 70:1–12. [PubMed: 15907809]
8. Pan JS, Hong MZ, Ren JL. Reactive oxygen species: a double edged sword in oncogenesis. World J Gastroenterol. 2009; 15:1702–1707. [PubMed: 19360913]
9. Sreedhar AS, Soti C, Csermely P. Inhibition of Hsp90: a new strategy for inhibiting protein kinases. Biochim Biophys Acta. 2004; 1697:233–242. [PubMed: 15023364]
10. Richter K, Buchner J. Hsp90: chaperoning signal transduction. J Cell Physiol. 2001; 188:281–290. [PubMed: 11473354]
11. Mann J. Natural products in cancer chemotherapy: past, present and future. Nat Rev Cancer. 2002; 2:143–148. [PubMed: 12635177]
12. Newman DJ, Cragg GM, Snader KM. The influence of natural products upon drug discovery. Nat Prod Rep. 2000; 17:215–234. [PubMed: 10888010]
13. Ramsewak RS, Nair MG, Strasburg GM, et al. Biologically active carbazole alkaloids from *Murraya koenigii*. J Agric Food Chem. 1999; 47:444–447. [PubMed: 10563914]
14. Tachibana Y, Kikuzaki H, Lajis NH, et al. Antioxidative activity of carbazoles from *Murraya koenigii* leaves. J Agric Food Chem. 2001; 49:5589–5594. [PubMed: 11714364]
15. Nakahara K, Trakoontivakorn G, Alzoreky NS, et al. Antimutagenicity of some edible Thai plants, and a bioactive carbazole alkaloid, mahanine, isolated from *Micromelum minsutum*. J Agric Food Chem. 2002; 50:4796–4802. [PubMed: 12166962]
16. Ito C, Itoigawa M, Nakao K, et al. Induction of apoptosis by carbazole alkaloids isolated from *Murraya koenigii*. Phytomedicine. 2006; 13:359–365. [PubMed: 16635744]

17. Roy MK, Thalang VN, Trakoontivakorn G, et al. Mahanine, a carbazole alkaloid from *Micromelum minsutum*, inhibits cell growth and induces apoptosis in U937 cells through a mitochondrial dependent pathway. Br J Pharmacol. 2005; 145:145–155. [PubMed: 15753952]
18. Roy MK, Thalang VN, Trakoontivakorn G, et al. Mechanism of mahanine-induced apoptosis in human leukemia cells (HL-60). Biochem Pharmacol. 2004; 67:41–51. [PubMed: 14667927]
19. Sinha S, Pal BC, Jagadeesh S, et al. Mahanine inhibits growth and induces apoptosis in prostate cancer cells through the deactivation of Akt and activation of caspases. Prostate. 2006; 66:1257–1265. [PubMed: 16683271]
20. Bhattacharya K, Samanta SK, Tripathi R, et al. Apoptotic effects of mahanine on human leukemic cells are mediated through crosstalk between Apo-1/Fas signaling and the Bid protein and via mitochondrial pathways. Biochem Pharmacol. 2010; 79:361–372. [PubMed: 19751707]
21. Jagadeesh S, Sinha S, Pal BC, et al. Mahanine reverses an epigenetically silenced tumor suppressor gene RASSF1A in human prostate cancer cells. Biochem Biophys Res Commun. 2007; 362:212–217. [PubMed: 17698033]
22. Mosman T. Rapid colorimetric assay for cellular growth and survival: application to proliferation and cytotoxicity assays. J Immunol Methods. 1983; 65:55–63. [PubMed: 6606682]
23. Bai J, Cederbaum AI. Catalase protects HepG2 cells from apoptosis induced by DNA-damaging agents by accelerating the degradation of p53. J Biol Chem. 2003; 278:4660–4667. [PubMed: 12468545]
24. Cumming RC, Andon NL, Haynes PA, et al. Protein disulfide bond formation in the cytoplasm during oxidative stress. J Biol Chem. 2004; 279:21749–21758. [PubMed: 15031298]
25. Csermely P, Kahn CR. The 90-kDa heat shock protein (hsp-90) possesses an ATP binding site and autophosphorylating activity. J Biol Chem. 1991; 266:4943–4950. [PubMed: 2002041]
26. Csermely P, Kajtár J, Hollósi M, et al. The 90 kDa heat shock protein (hsp90) induces the condensation of the chromatin structure. Biochem Biophys Res Commun. 1994; 202:1657–1663. [PubMed: 8060353]
27. Zhang T, Hamza A, Cao X, et al. A novel Hsp90 inhibitor to disrupt Hsp90/Cdc37 complex against pancreatic cancer cells. Mol Cancer Ther. 2008; 7:162–170. [PubMed: 18202019]
28. Ghoshal A, Mukhopadhyay S, Deminse R, et al. Detection and characterization of a sialoglycosylated bacterial ABC-type phosphate transporter protein from patients with visceral leishmaniasis. Glycoconj J. 2009; 26:675–689. [PubMed: 19184417]
29. Morris GM, Huey R, Lindstrom W, et al. AutoDock4 and AutoDockTools4: automated docking with selective receptor flexibility. J Comput Chem. 2009; 30:2785–2791. [PubMed: 19399780]
30. Van der Spoel D, Lindahl E, Hess B, et al. GROMACS: fast, flexible, and free. J Comput Chem. 2005; 26:1701–1718. [PubMed: 16211538]
31. Lu SY, Jiang YJ, Lv J, et al. Molecular docking and molecular dynamics simulation studies of GPR40 receptor-agonist interactions. J Mol Graph Model. 2010; 28:766–774. [PubMed: 20227312]
32. Schüttelkopf AW, Van Aalten DM. PRODRG: a tool for high-throughput crystallography of protein-ligand complexes. Acta Crystallogr D Biol Crystallogr. 2004; 60:1355–1363. [PubMed: 15272157]
33. Humphrey W, Dalke A, Schulten K. VMD— visual molecular dynamics. J Mol Graph. 1996; 14:33–38. [PubMed: 8744570]
34. Aqvist J, Marelius J. The linear interaction energy method for predicting ligand binding free energies. Comb Chem HighThroughput Screen. 2001; 4:613–626.
35. Aqvist J, Luzhkov VB, Brandsdal BO. Ligand binding affinities from MD simulations. Acc Chem Res. 2002; 35:358–365. [PubMed: 12069620]
36. Hansson T, Aqvist J. Estimation of binding free energies for HIV proteinase inhibitors by molecular dynamics simulations. Protein Eng. 1995; 8:1137–1144. [PubMed: 8819979]
37. Seeliger D, de Groot BL. Ligand docking and binding site analysis with PyMOL and Autodock/Vina. J Comput Aided Mol Des. 2010; 24:417–422. [PubMed: 20401516]
38. Liang CC, Park AY, Guan JL. *In vitro* scratch assay: a convenient and inexpensive method for analysis of cell migration *in vitro*. Nat Protoc. 2007; 2:329–333. [PubMed: 17406593]

39. Sipos B, Möser S, Kalthoff H, et al. A comprehensive characterization of pancreatic ductal carcinoma cell lines: towards the establishment of an in vitro research platform. Virchows Arch. 2003; 442:444–452. [PubMed: 12692724]
40. Fan TJ, Han LH, Cong RS, et al. Caspase family proteases and apoptosis. Acta Biochim Biophys Sin (Shanghai). 2005; 37:719–727. [PubMed: 16270150]
41. Clark CB, Rane MJ, El Mehdi D, et al. Role of oxidative stress in geldanamycin-induced cytotoxicity and disruption of Hsp90 signaling complex. Free Radic Biol Med. 2009; 47:1440–1449. [PubMed: 19703551]
42. Fukuyo Y, Inoue M, Nakajima T, et al. Oxidative stress plays a critical role in inactivating mutant BRAF by geldanamycin derivatives. Cancer Res. 2008; 68:6324–6330. [PubMed: 18676857]
43. Chen G, Zhang X, Zhao M, et al. Celastrol targets mitochondrial respiratory chain complex I to induce reactive oxygen species-dependent cytotoxicity in tumor cells. BMC Cancer. 2011; 11:170–182. [PubMed: 21569548]
44. Tsutsumi S, Beebe K, Neckers L. Impact of heat-shock protein 90 on cancer metastasis. Future Oncol. 2009; 5:679–688. [PubMed: 19519207]
45. Ogata M, Naito Z, Tanaka S, et al. Overexpression and localization of heat shock proteins mRNA in pancreatic carcinoma. J Nippon Med Sch. 2000; 67:177–185. [PubMed: 10851351]
46. Richardson PG, Mitsiades CS, Laubach JP, et al. Inhibition of heat shock protein 90 (HSP90) as a therapeutic strategy for the treatment of myeloma and other cancers. Br J Hematol. 2011; 152:367–379.
47. Eccles SA, Massey A, Raynaud FI, et al. NVPAUY922: a novel heat shock protein 90 inhibitor active against xenograft tumour growth, angiogenesis, and metastasis. Cancer Res. 2008; 68:2850–2860. [PubMed: 18413753]
48. Rao RV, Niazi K, Mollahan P, et al. Coupling endoplasmic reticulum stress to the cell-death program: a novel HSP90-independent role for the small chaperone protein p23. Cell Death Differ. 2006; 13:415–425. [PubMed: 16195741]

What's new?

Pancreatic cancer is lethal and often shows resistance to conventional chemotherapy. New drugs and/or combinations of drugs are required for greater efficacy as well as to overcome the observed chemoresistance. Hsp90 is highly expressed in cancerous cells for their survival, making it a potential chemotherapy target. ROS is a critical mediator of apoptosis and can lead to Hsp90 dysfunction. Our data demonstrate the involvement of mahanine-induced ROS in Hsp90 dysfunction which leads to a subsequent disruption of the Hsp90-Cdc37 chaperone complex in pancreatic cancer.

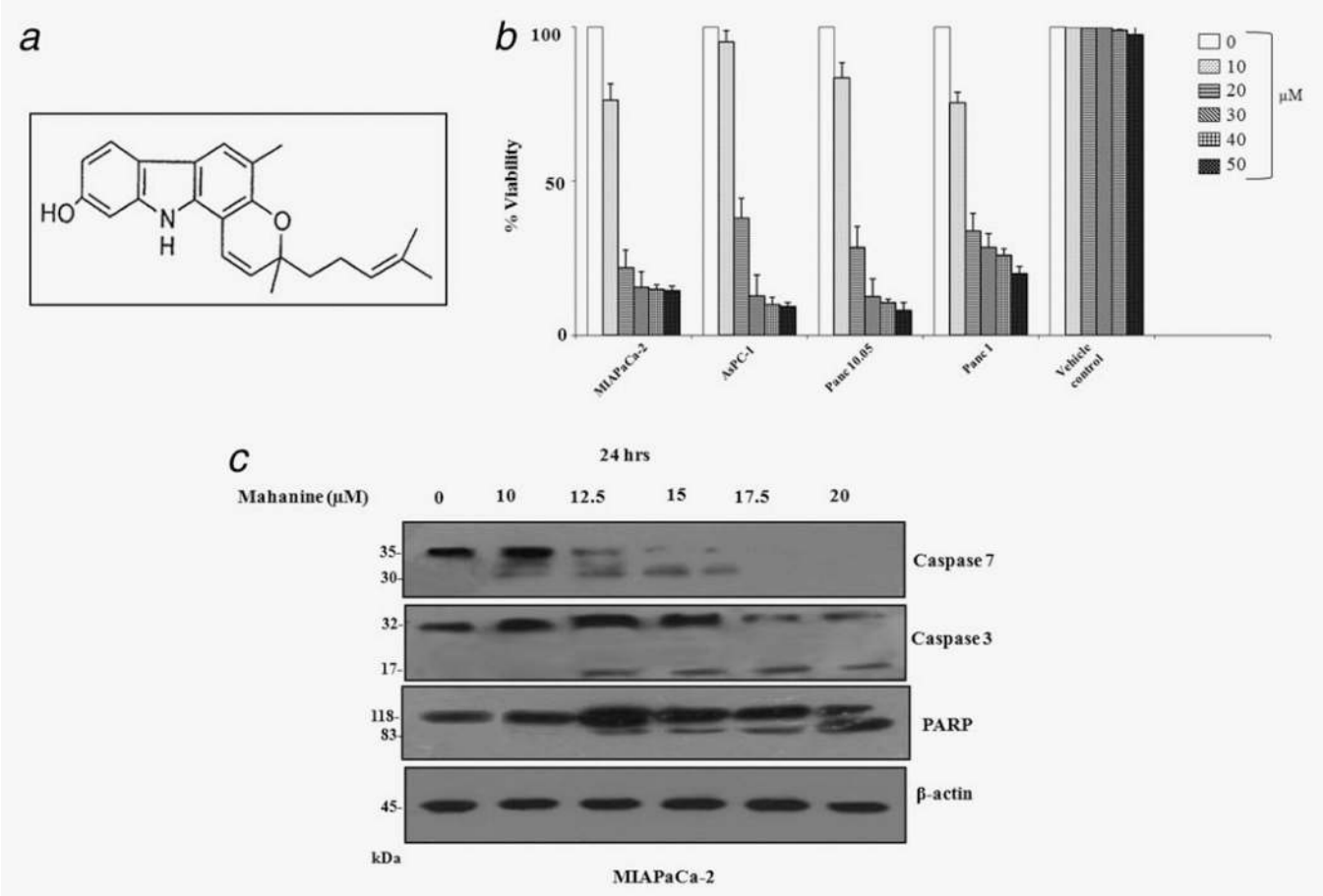

Figure 1.

Mahanine-induced apoptosis in pancreatic cancer cells. (*a*) Chemical structure of mahanine, a carbazole alkaloid. (*b*) Mahanine-induced decrease in pancreatic adenocarcinoma cell viability measured by MTT assay after 48 hr. Cell viability was represented as % viability. Each value is the mean ± SD of three independent experiments. (*c*) Mahanine induced positive regulation of known molecular mediators of apoptosis in MIAPaCa-2 after 24 hr incubation, analyzed by Western blotting.

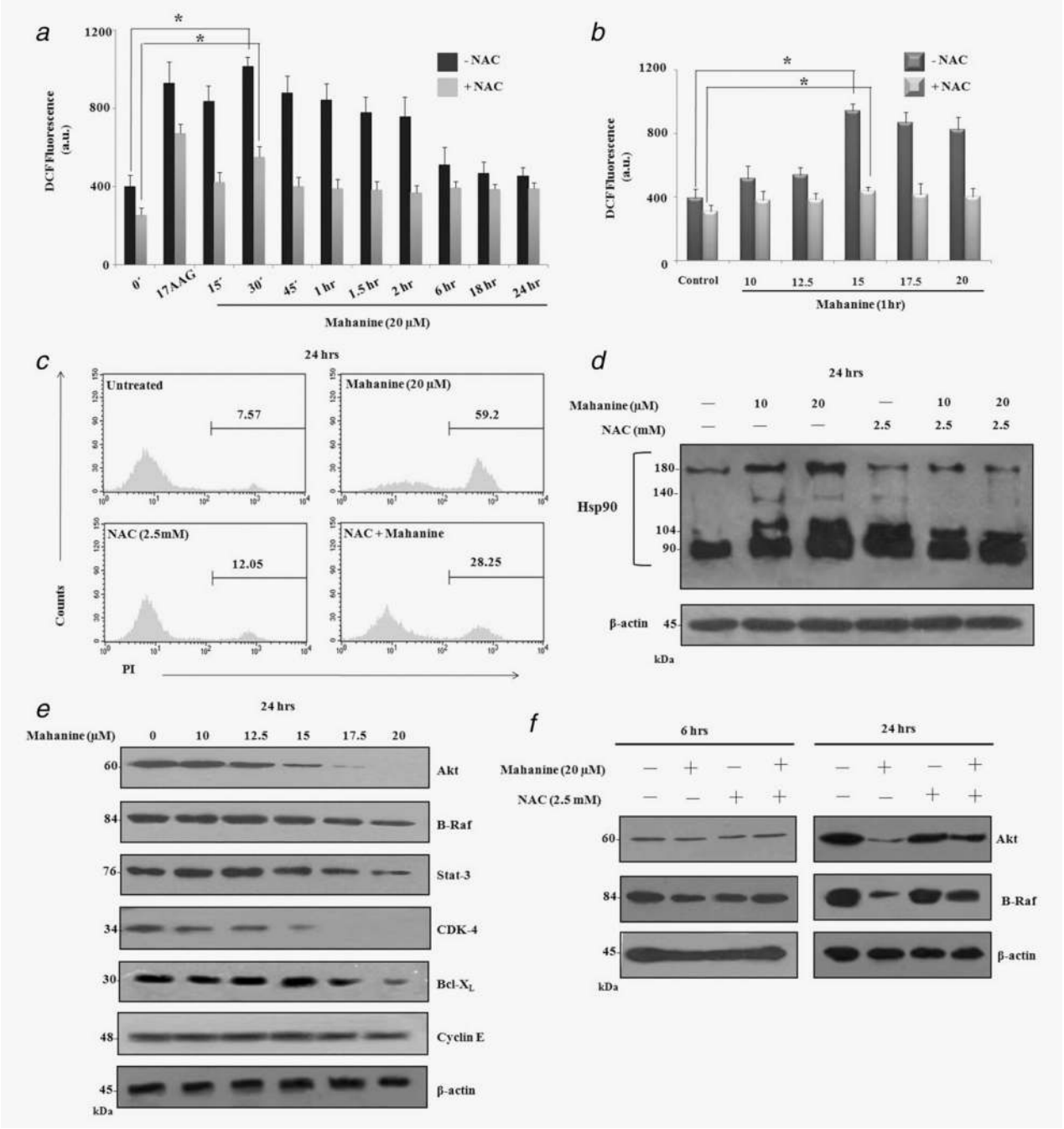

Figure 2.

Mahanine induces ROS accumulation in both a time- and dose-dependent manner, leading to Hsp90 dysfunction in MIAPaCa-2 cells. MIAPaCa-2 cells were subjected to 20 μM mahanine treatment for 0–24 hr. ROS production was measured by H_2DCF-DA staining and was inhibited by 1 hr pretreatment of cells with NAC (2.5 mM). The17-AAG (1 μM) was used as a positive control. The results are expressed as MFI (a.u.) Each value is the mean ± SD of three independent experiments. "*" indicates $p < 0.05$. MIAPaCa-2 cells were subjected to mahanine (10–20 μM) treatment for 1 hr and processed as above. Each value is the mean ± SD of three independent experiments. "*" indicates a significant difference of p

< 0.05. NAC (2.5 mM) treatment for 1 hr prevented the effect of 20 μM mahanine on cell viability, as reflected in the decrease of PI positivity by flow cytometric analysis after 24 hr. Mahanine-induced ROS-mediated Hsp90 dysfunction in MIAPaCa-2 cells. MIAPaCa-2 cells were treated with mahanine (10 and 20 μM) for 24 hr after preincubation without or with NAC (2.5 mM, for 1 hr). Experiments were performed as described in the Material and Methods section. Mahanine-induced ROS generation led to disulfide linkage of Hsp90, as shown by the slower migration rate on nonreducing SDS-PAGE, concentrated in higher molecular weight regions, which was ameliorated by subsequent NAC incubation. Mahanine downregulates the Hsp90 client proteins levels. MIAPaCa-2 cells were subjected to mahanine treatment for 24 hr and analyzed by Western Blot with the indicated antibodies. A dose-responsive decrease in the Hsp90 client protein levels in MIAPaCa-2 cells, whereas no down-regulation was observed in nonclient protein Cyclin E. ROS-dependent down regulation of Hsp90 client proteins. NAC-pre-treated (2.5 mM) MIAPaCa-2 cells were incubated with mahanine (20 μM) for 6 and 24 hr, respectively, and analyzed by Western Blot with the indicated antibodies. The presented data have been derived from three different experiments, one of which is shown here.

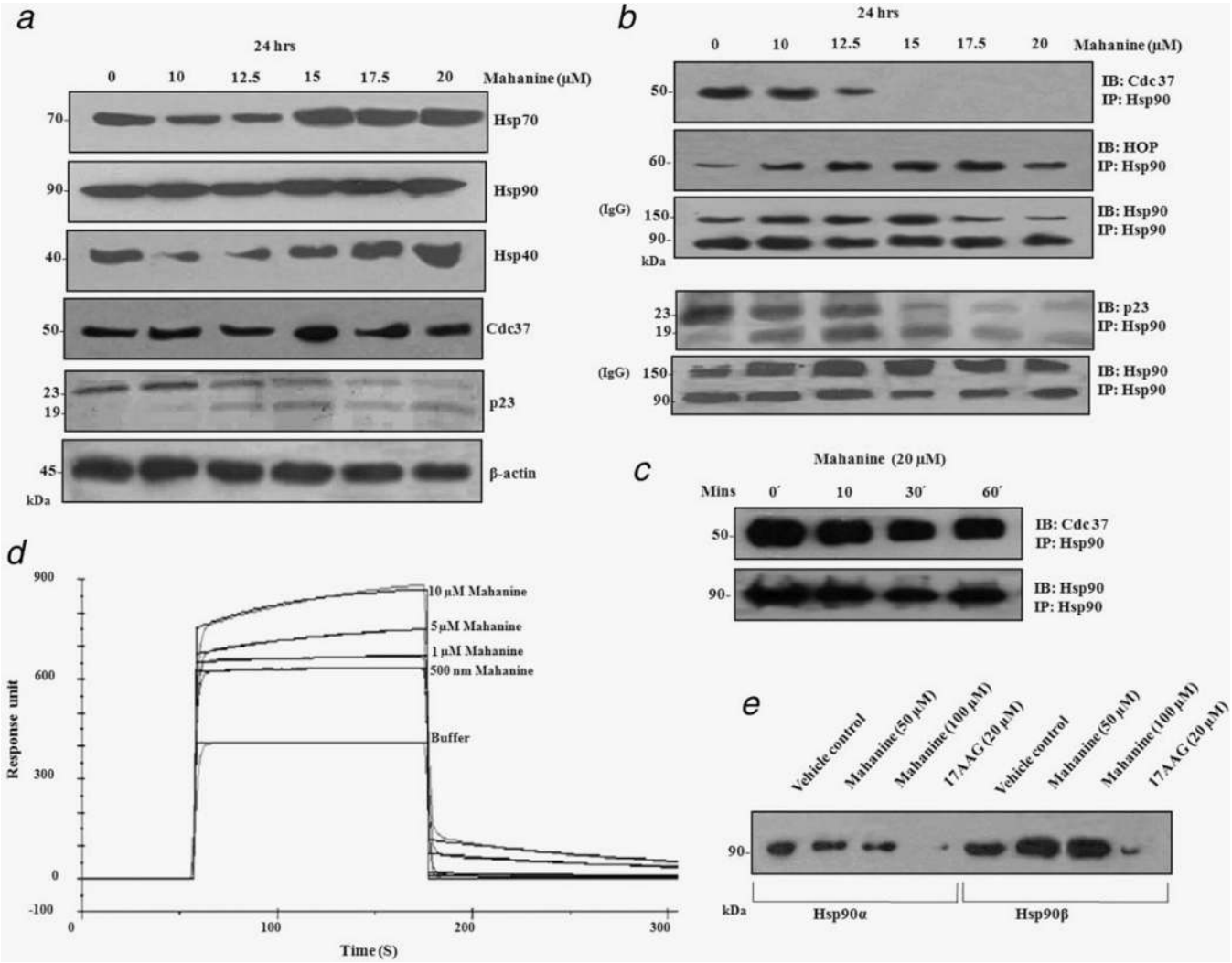

Figure 3.

(*a*) Differential regulation of Hsp90 cochaperones after mahanine treatment. MIAPaCa-2 cells were subjected to mahanine treatment for 24 hr and whole cell lysate was analyzed by Western blot with the specified antibodies. Mahanine induced Hsp70 and Hsp40 upregulation. The total protein level of Cdc37 remained unaltered, whereas p23 was cleaved from 23 to 19 kDa. The data is shown as a representative example of three separate experimental data sets. (*b*) Mahanine dissociates Cdc37, but not HOP from the Hsp90 super-chaperone complex. MIAPaCa-2 cells were incubated with mahanine for 24 hr and immunoprecipitated with an anti-Hsp90 antibody. The resulting immune-complex was resolved on SDS-PAGE, and was subsequently identified by anti-Cdc37, anti-HOP and anti-p23 antibodies followed by ECL-mediated detection. Mahanine dissociated Cdc37, but not HOP or p23, from the Hsp90 super-chaperone complex. The data are representative of three individual experiments. (*c*) Mahanine does not dissociate the Cdc-37-Hsp90 super-chaperone complex at an early time point of ROS generation. MIAPaCa-2 cells were incubated with mahanine for 10–60 min and immunoprecipitated as described above. The data represent three individual experiments. (*d*) SPR study of mahanine with recombinant Hsp90. Various doses of mahanine (0.5, 1, 5, 10 μM) were added to immobilized human Hsp90 at a final concentration of 50 μg ml^{-1}. The coupling of Hsp90 to the CM5 sensor chip and measurement of SPR were performed as described in the Material and Methods section.

(*e*) The ATP binding of Hsp90 was not hindered by mahanine induction. Recombinant human Hsp90α (5 μg) and Hsp90β (5 μg) were incubated with mahanine (50 and 100 μM) and 17-AAG (20 μM, a known Hsp90 inhibitor) in incubation buffer for 30 min, as described in Material and Methods. Subsequently, ATP-Sepharose (25 μl) were added to the reaction mixture to pull down Hsp90, and analyzed by Western blotting using an anti-Hsp90 antibody. The assay revealed that successive doses of mahanine did not hamper ATP binding with purified Hsp90α and Hsp90β, whilst 17AAG was able to do so.

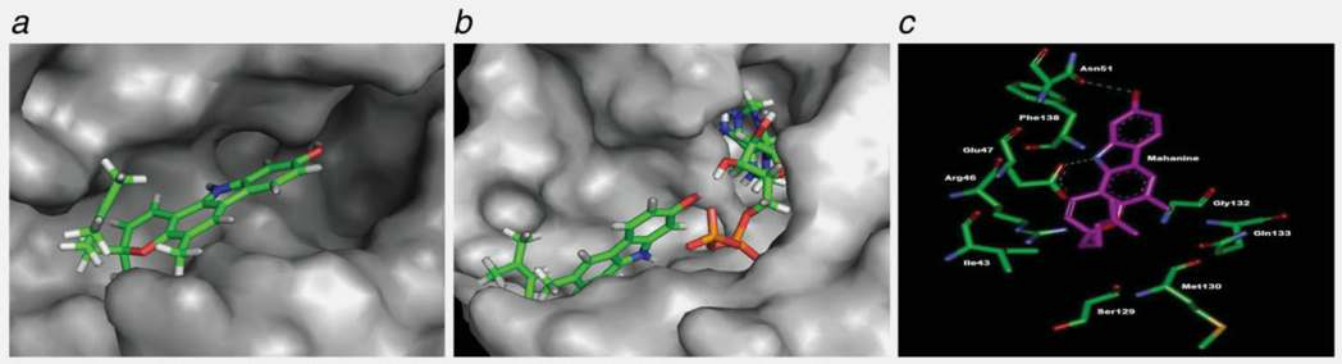

Figure 4.

Molecular modeling studies of Hsp90-mahanine interaction. (*a*) Binding site of mahanine in Hsp90. Mahanine is displayed in a stick model and Hsp90 in a surface view. (*b*) Status of mahanine and ATP in Hsp90. Surface representation of Hsp90 with mahanine and ATP in a stick model. (*c*) Residues involved in the interaction of mahanine with Hsp90. Hsp90 and mahanine are represented in a stick model; the sticks are colored according to the type of atom. Carbon = green in Hsp90 and pink in Cdc37. [Color figure can be viewed in the online issue, which is available at wileyonlinelibrary.com.]

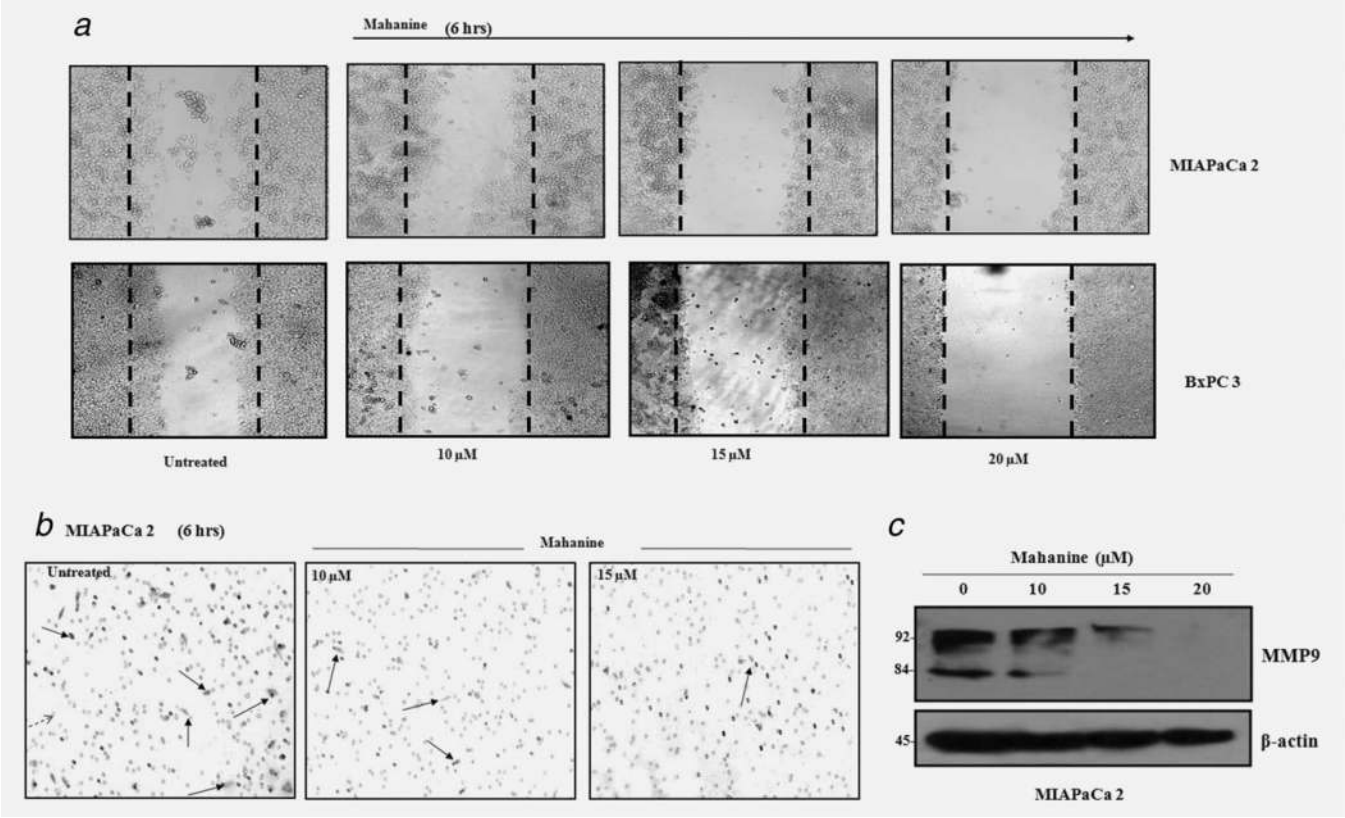

Figure 5.

Mahanine-mediated inhibition of cell haptotaxis and chemo-migration in pancreatic adenocarcinoma. (*a*) MIAPaCa-2 and BxPC-3 cells were grown to confluency in six-well plates; subsequently scratches were made, followed by incubation without or with mahanine for 6 hr. Cells showed >40% cell migration (cell haptotaxis) in the vehicle control, whereas the highest treatment dose resulted in <5% migratory cells, as shown by phase-contrast microscopy. (*b*) Mahanine untreated and treated MIAPaCa-2 cells were exposed to EGF (20 ng ml^{-1}) in a transwell plate, as described in Material and Methods, and incubated for 6 hr. Cells exhibited a dose-dependent decline in EGF-driven chemo-migration. (*c*) Mahanine reduces MMP9 in MIAPaCa-2 cells. MIAPaCa-2 cells incubated for 24 hr in the absence and presence of mahanine, and whole cell lysate was analyzed by Western blot with an anti-MMP9 antibody. [Color figure can be viewed in the online issue, which is available at wileyonlinelibrary.com.]

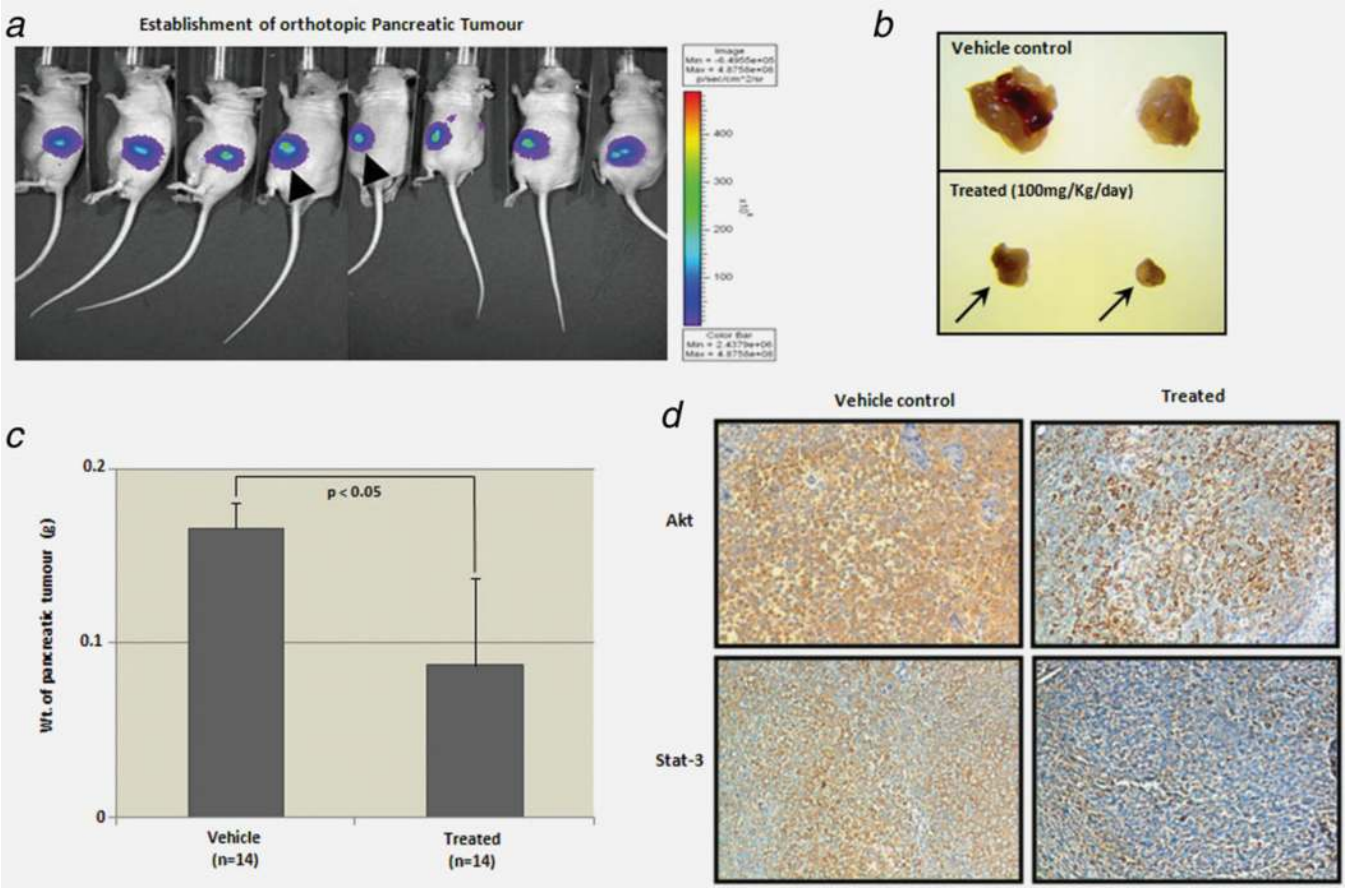

Figure 6.

Mahanine inhibits pancreatic tumors in an orthotopic nude mouse model. (*a*) Luciferase containing MIAPaCa-2 cells were implanted into the pancreas of athymic nude mice to generate pancreatic tumors orthotopically. Establishment of orthotopic pancreatic tumors in immunodeficient athymic nu/nu mice before starting the treatment was confirmed by *in vivo* bioluminsescent imaging (Supporting Information Fig. S-10) and a representative figure is given. (*b*) Reduction of tumor mass as reflected by two representative pancreatic tumors excised after 12 days of vehicle (control) and mahanine treatment (i.p., 100 mg/kg/day). (*c*) Pancreatic tumor load represented as the weight of the tumor after excision from the pancreas, in the control and treated groups. The tumor load was significantly lower in the mahanine-treated than the vehicle-treated group. "*" indicates $p < 0.05$. (*d*) The Akt and Stat-3 protein levels were determined by immunohistochemistry staining in the tumor orthograft control and treated tissue samples. [Color figure can be viewed in the online issue, which is available at wileyonlinelibrary.com.]